



RESEARCH ARTICLE

INVERTED BRAYTON CYCLE ENGINE OPTIMIZATION FOR HYPERSONIC FLIGHT

Mustafa KARABACAK^{1,*} , Önder TURAN² 

¹ Department of Aeronautical Engineering, Faculty of Aeronautics and Astronautics, Necmettin Erbakan University, Konya, TR- 42140, Turkey

² Department of Airframe and Powerplant Maintenance, Faculty of Aeronautics and Astronautics, Eskişehir Technical University, Eskişehir, TR-26470, Turkey

ABSTRACT

The objectives of this study are to determine the optimum design parameters of a IBCE for hypersonic flight and to investigate the relationship between engine performance and design parameters. The investigation of these objectives is made first in the literature in this study. The optimization of inverted Brayton cycle engine ,IBCE, is performed using the particle swarm optimization method in this study. The optimum specific thrust, sT , value is reached by staying within the optimization constraints. When the total temperature of the cooling section is examined, a temperature above the freezing temperature of the air is obtained. A very high sT value, 451 N.s/kg is obtained at the hypersonic flight Mach Number (5 Mach) as a result of optimization. By the investigation, it is concluded that specific fuel consumption, SFC, reduces % 5.3 and sT increases % 5.6 dependent on preburner exit total temperature, PETT, change from 2100 K to 1400 K. Based on total temperature decrease at cooling section, $T_{cooling}$, change from 100 K to 500 K, it is seen that by the investigation, SFC increases %23.7 and sT increases % 13.1. It is seen that SFC reduces by % 6.3 and sT increases by % 35.9 depending on afterburner exit total temperature, AETT, change from 2000 K to 2300 K. It is observed that SFC reduces % 10.5 and sT increases % 11.7 dependent on total pressure ratio of turbine, π_t , change from 0.9 to 0.1.

Keywords: Jet engine, Optimization, Hypersonic flight, Inverted Brayton cycle, Engine performance

NOMENCLATURE

Abbreviations

AETT	Afterburner Exit Total Temperature
IBCE	Inverted Brayton Cycle Engine
PETT	Preburner Exit Total Temperature
SFC	Specific Fuel consumption (unit: g/(kN.s))

Greek Letters

τ	Total temperature ratio
π	Total pressure ratio

Latin Symbols

a	Sound speed (unit m/s)
c	Specific heat (unit: J/(kg.K))
K	Kelvin
m	Mass flow rate (unit: kg/s)
M	Flight Mach Number
$M_{flightlimit}$	Maximum Flight Mach Number thrust can be generated
N	Newton (unit: kg.m/s ²)
P	Pressure (unit: N/m ²)
R	Molar gas constant (unit: J/(K.kg))
s	Second
sT	Specific Thrust (unit: (m/s))

*Corresponding Author: karabacak7@itu.edu.tr

Received: 25.03.2023 Published: 27.12.2023

T	Temperature (unit: K)
$T_{cooling}$	Total temperature decrease at cooling section
$T_{c\,limit}$	Total temperature limit of engine gas flow at compressor exit
$T_{flow\,limit}$	Total temperature limit of engine gas flow at specific engine section
$T_{material\,limit}$	Material temperature limit
$T_{n\,limit}$	Total temperature limit of engine gas flow at nozzle inlet
$T_{t\,combuster\,exit\,limit}$	Combustors exit total temperature limit of gas flow
$T_{t\,limit}$	Total temperature limit of engine gas flow at burner exit
$T_{t\,flow\,limit}$	Allowable total temperature limit of engine gas flow
$T_{t\,cooling}$	Engine gas flow total temperature decrease at cooling section
V_{flight}	Flight velocity
y	Specific heat ratio

Subscripts

a	Ambient
p	Constant pressure

Superscripts

afterburner	Afterburner
c	Compressor
preburner	Preburner
t	Total, Turbine
total	Total
1,2,3...	Engine section that expressed in nomenclature

1. INTRODUCTION

Engineering design concepts are created with the expectation of meeting the requirements of the engineering discipline [1,2]. While some engineering design concepts achieve success during the design period, many engineering design concepts have to wait until they are used in the engineering world related to their discipline [3,4]. However, whether engineering design concepts succeed on time or wait for the time when they will be applied to current practice, the maturation process of engineering design must begin in order to achieve success [5]. However, concepts with a waiting period requirement for applicability usually require a longer and more challenging maturity process.

IBCE is a concept that is categorized as a concept that requires a waiting period before it can be implemented [6]. During the maturity process of engineering design, the concept needs to be optimized to more adequately meet the design requirements depending on the design conditions [7,8]. Aviation design concepts are unexceptional with respect to maturity process requirements. To ensure a feasible design, aeronautical design concepts, such as jet engine concepts, should be optimized [9-11].

The design conditions are flight conditions for aero engines and the ICCE is expected to be used for hypersonic flight propulsion. Therefore, the ICCE should be optimized to meet the hypersonic flight requirements. To meet the hypersonic flight requirement, the IBCE concept is expected to provide sufficient thrust to overcome the enormous drag caused by hypersonic flight. Conventional engines cannot produce thrust or sufficient thrust in hypersonic flight, so engines used to propel hypersonic vehicles can produce sufficient thrust in hypersonic flight, and IBCE is a suitable candidate for these conditions.

It is expected that with the intercooled turbofan concept, the SFC is reduced and the thermal efficiency is increased [12,13]. Precooled cycles, such as the ATREX [14], the SABRE [15] and Scimitar [16] have been developed for the vision of next-generation low-cost transportation [17]. The state-of-the-art heat exchanger and manufacturing technology were investigated by Murray et al [18], and it was

concluded that heat exchangers based on current technology level are not sufficient for the aviation industry [17]. Using an inverted Brayton cycle to recover thermal energy from exhaust gas is a novel technological option that has not been widely discussed [19]. In the investigation of Kennedy et al [20], inverted Brayton cycle-based application on a reciprocating internal combustion engine was studied on a preliminary experimental setup for a gasoline engine; nevertheless, this is the only experimental conduct developed for this concept [19]. Besides, this concept expressed is also used to generate supersonic and hypersonic propulsion. The use of ramjet engine and scramjet engines to generate thrust for supersonic and hypersonic propulsion has been widely investigated. Generation of sufficient thrust through heat addition at supersonic speeds is still a challenging task due to the residence time of the supersonic speed in scramjet combustors is only a few milliseconds [21,22] Shock waves and fuel entrainment's coupled effect phenomena are required to perform plenty of situations efficiently [23,24,25] and to discover more [26]. Few of these coupled effect phenomenon transitions have been analyzed by researchers of supersonic flow engines. Although it has been working in the field of scramjet for a long time, the lack of required maturity in this field still shows that new engine concepts required to be investigated on. IBCE for higher speed aero vehicle which is a novel technological option that has not been investigated enough in the literature for reaching required maturity, is investigated in this study. Zhang et al. [27] studied exergy analysis and optimization of an inverted Brayton cycle and indicated that exergy loss of combustion in the cycle is the largest and followed by heat exchanger.

1.1. The Novelty of the Study

This study focuses on the optimization of IBCE to provide hypersonic flight. IBCE optimization is the first step in this study. First, in the literature, IBCE performance investigation dependent on design parameters is made in this study. Equations for IBCE are derived and demonstrations of these equations are made firstly in this study. Performance analysis depends on design parameters and design conditions are discussed in detail in this study firstly. The conventional particle swarm optimization algorithm firstly applied IBCE optimization in this study and the application of the particle swarm optimization algorithm on IBCE optimization is the novelty of this study.

The main novelties of this study are expressed as follows,

- IBCE performance investigation based on the design parameters of engine firstly made in this study.
- IBCE optimization for hypersonic flight is made in this study firstly.
- The particle swarm algorithm is applied to engine optimization for hypersonic flight subject firstly in this study.

2. SYSTEM DESCRIPTION

The IBCE components are illustrated in Figure 1 [28].

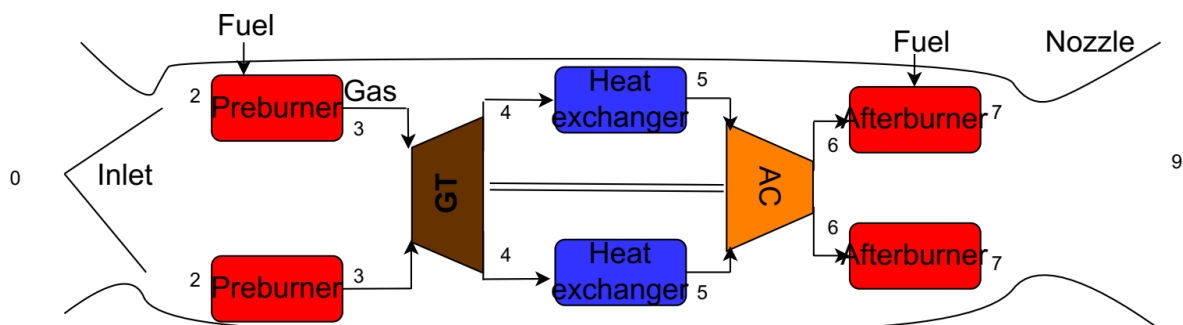


Figure 1. IBCE scheme and nomenclature [28]

Assumed that IBCE is ideal as expressed in Table 1 in more detail in this study.

Diffuser section reduces air flow velocity to the value that is suitable for preburner and later engine sections; preburner section increase total temperature of flow by using combustion energy; turbine section uses energy of flow to work compressor and so flow total temperature and flow total pressure reduce; heat exchanger or cooling section reduce total temperature of flow at constant flow total pressure to increase compressor exit total pressure; compressor increases total pressure and total temperature of flow and works by turbine power; afterburner increases total temperature of flow at constant flow total pressure; nozzle increases velocity of flow with reduce static pressure of flow and nozzle reduces static pressure of flow to value that is equal atmosphere pressure to obtain maximum thrust and minimum SFC on ideal conditions.

The assumptions for the engine system used in this study are expressed as,

- Isentropic compressor and turbine
- Constant pressure combustion and cooling
- No energy losses in the system
- No losses in the nozzle and diffuser
- % 100 combustion efficiency
- Constant flow characteristics
- The fuel mass flow rate is neglected.
- Optimum expansion in the nozzle

2.1. The Mathematical Model of the IBCE

The components of the IBCE concept and the nomenclature of the engine concept are shown in Figure 1.

The equations used to determine sT and SFC of the ideal IBCE dependent on the nomenclature shown in Figure 1 are expressed in Equations. (1) – (33).

It is assumed that the inlet flow Mach Number is equal to the flight Mach Number and by applying the isentropic relations of total temperature and total pressure at the inlet expressed as follows:

$$P_{t_0} = P_a \times \left(1 + \frac{\gamma - 1}{2} \times M^2 \right)^{\frac{\gamma}{\gamma - 1}} \quad (1)$$

$$T_{t_0} = T_a \times \left(1 + \frac{\gamma - 1}{2} \times M^2 \right) \quad (2)$$

Inlet flow pressure losses occur due to the viscosity of air and friction at the inlet solid layer between air flow and due to the shock generation due to the supersonic and hypersonic flow in this study, it is assumed that the ideal engine that is no losses of the pressure as described equation:

$$P_{t_2} = P_{t_0} \quad (3)$$

In the inlet heat flow between the inlet wall and the atmosphere, so it is expected that total temperature losses occur, but according to the ideal engine assumptions, there are no losses of total temperature at the inlet as shown in equation:

$$T_{t_2} = T_{t_0} \quad (4)$$

Turbulence is the desired state for combustion because of air and fuel mixing requirements. On the other hand, turbulence flow during combustion leads to total pressure losses, but in this study, losses are neglected as expressed in equation:

$$P_{t_3} = P_{t_2} \quad (5)$$

PETT is limited by the turbine section total temperature limit defined as;

$$T_{t_3} = T_{t_{limit}} \quad (6)$$

The turbine total temperature ratio is defined by isentropic relations by applying the isentropic turbine assumption as follows:

$$\zeta_t = \pi_t^{\frac{\gamma-1}{\gamma}} \quad (7)$$

The turbine exit total temperature depends on the total temperature ratio of the turbine, is expressed below:

$$T_{t_4} = T_{t_3} \times \zeta_t \quad (8)$$

It is assumed that the total pressure losses at the cooling section are neglected as determined by the following equation:

$$P_{t_5} = P_{t_4} \quad (9)$$

To reach a higher total pressure at the compressor exit, cooling is applied at the cooling section. Compressor inlet total temperature is dependent on the total temperature decrease at the cooling section as expressed as follows:

$$T_{t_5} = T_{t_4} - T_{t_{cooling}} \quad (10)$$

The energy balance between the turbine and compressor by applying assumption that the fuel flow rate is neglected and the specific heat, c_p , is constant, is defined as the follows:

$$m \times c_p \times (T_{t_3} - T_{t_4}) = m \times c_p \times (T_{t_6} - T_{t_5}) \quad (11)$$

The compressor exit total temperature based on the energy balance between the turbine and compressor is expressed:

$$T_{t_6} = (T_{t_3} - T_{t_4}) + T_{t_5} \quad (12)$$

The compressor total temperature ratio, ζ_c , dependent on compressor exit total temperature, T_{t_6} , and compressor inlet total temperature, T_{t_5} , determined as the following:

$$\zeta_c = \frac{T_{t_6}}{T_{t_5}} \quad (13)$$

Compressor total pressure ratio, π_c , is expressed by applying the isentropic compressor assumption, by isentropic relations as,

$$\pi_c = \zeta_c^{\frac{\gamma}{\gamma-1}} \quad (14)$$

Compressor exit total pressure, P_{t_6} , dependent on compressor total pressure ratio and compressor inlet total pressure, expressed as the following:

$$P_{t_6} = P_{t_5} \times \pi_c \quad (15)$$

$$T_{t_6} < T_{c_{limit}} \quad (16)$$

Similar to the preburner, afterburner exit total pressure equals the afterburner inlet total pressure as shown,

$$P_{t_7} = P_{t_6} \quad (17)$$

Similar to the preburner, the AETT is limited by the nozzle section total temperature limit as defined as,

$$T_{t_7} = T_{n_{limit}} \quad (18)$$

Similar to the inlet, there is heat flow between the nozzle wall and the atmosphere and heat losses due to the shock generation; therefore, it is expected that total temperature losses occur, but according to the ideal engine assumption, there are no losses of total temperature at the inlet as shown in equation:

$$T_{t9} = T_{t7} \quad (19)$$

Similar to the inlet, nozzle flow pressure losses occur, due to the viscosity of air and friction between the nozzle solid layer and air flow and due to the shock generation because of the supersonic and hypersonic flow in the nozzle. However, in this study, it is assumed that the ideal engine has no flow losses of the pressure, as expressed by the equation:

$$P_{t9} = P_{t7} \quad (20)$$

It is assumed that the optimum expansion in the nozzle so that nozzle exit static pressure expands to the ambient pressure, as expressed in equation,

$$P_9 = P_a \quad (21)$$

The nozzle exits flow Mach Number and static temperature, determined by the isentropic relation as expressed,

$$M_9 = \sqrt{\frac{2}{\gamma-1} \times \left(\frac{P_{t9}}{P_9} \frac{\gamma-1}{\gamma} - 1 \right)} \quad (22)$$

$$T_9 = \frac{T_{t9}}{1 + \frac{\gamma-1}{2} \times M_9^2} \quad (23)$$

Sound speed at nozzle exit condition and ambient conditions, and flow velocity of gas at nozzle exit and flow velocity at the engine inlet, which are dependent on sound speed, are calculated as expressed in the following equations,

$$a_9 = \sqrt{\gamma \times R \times T_9} \quad (24)$$

$$V_9 = a_9 \times M_9 \quad (25)$$

$$a_a = \sqrt{\gamma \times R \times T_a} \quad (26)$$

$$V_0 = M_0 \times a_a \quad (27)$$

The sT is determined depending on the flow velocity at the nozzle exit, V_9 , and inlet entrance, V_0 , and by applying the optimum expansion in the nozzle as,

$$sT = V_9 - V_0 \quad (28)$$

Engine flow energy level increasing between the combustor inlet and exit, is caused by the combustion of fuel so by applying this energy balance the fuel mass flow rate is estimated. It is assumed that the specific heat does not change due to the chemical reaction in the combustor. The fuel mass flow rate is at a very low level relative to the engine mass flow rate so it is neglected. All fuel that is mixed with air cannot be burned due to the imperfect mixing, but in this study, it is assumed that all fuel that is sprayed, be burned with air. Preburner, afterburner and total fuel mass flow rate is determined as,

$$m_{f_{preburner}} = \frac{m \times c_p \times (T_{t3} - T_{t2})}{Q_R} \quad (29)$$

$$m_{f_{afterburner}} = \frac{m \times c_p \times (T_{t7} - T_{t6})}{Q_R} \quad (30)$$

$$m_{f_t} = m_{f_{afterburner}} + m_{f_{preburner}} \quad (31)$$

Q_R , is the fuel heat-release rate level per unit fuel mass flow rate. The unit heat release is caused by fuel combustion, and the fuel mass flow rate is determined by the burner entrance and exit flow energy level and the heat of the fuel.

Thrust, T , depends on the sT and mass flow rate. SFC depends on the total fuel-mass flow rate, m_{ft} , and thrust. These are expressed as,

$$T = sT \times m \tag{32}$$

$$sfc = \frac{m_{ft}}{T} \tag{33}$$

3. INVESTIGATION OF THE EFFECT OF DESIGN PARAMETERS ON ENGINE PERFORMANCE

The base engine design parameter values and values of design conditions used to plot graphs that show the effect of design parameters on engine performance, are expressed at Table 1.

Table 1 Base engine design parameters

Design Parameters	Parameter Value
PETT	2050 K
π_t	0.1
$T_{cooling}$	400 K
AETT	2200 K
Flight Mach Number	5 Mach
Flight Altitude	11 km

3.1. PETT Effect on Engine Performance

sT reduces and SFC increases with PETT increases as shown in Figures 2 and 3 and this situation shows that reduce PETT increase performance. To obtain the best performance, PETT can reduce to a value that combustion do not be occurred and this value equals the diffuser exit total temperature that is expressed in Equation 34.

$$T_{t_0} = T_a \times \left(1 + \frac{\gamma - 1}{2} \times M^2 \right) \tag{34}$$

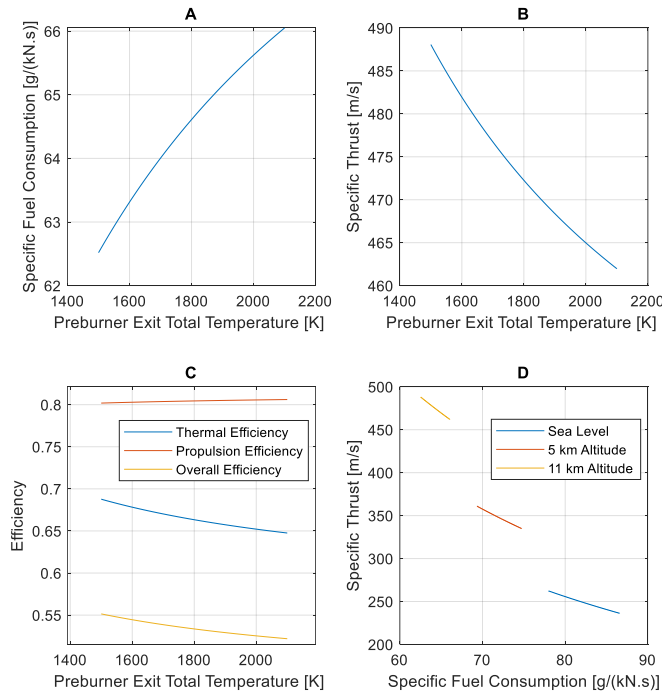


Figure 2. (A) SFC changes with PETT change (B) sT changes with PETT change (C) Engine efficiencies change with PETT (D) sT -SFC change with PETT at different altitudes

As can be observed in Figure 2 (A), the SFC decrease from 66.050 [g/(kN.s)] at 2100 K PETT to 62.518 [g/(kN.s)] at 1400 K PETT. The sT increase from 462.0 [m/s] at 2100 K PETT to 488.1 [m/s] at 1400 K PETT as shown in Figure 2 (B).

As seen in Figure 2 (C), the propulsion efficiency is 0.8019 at 1400 K PETT and 0.8061 at 2100 K PETT. Thus, the PETT has no significant effect on the thrust efficiency. The thermal efficiency is 0.6877 at 1400 K PETT and decreases to 0.6475 at 2100 K PETT. The overall efficiency decreases from 0.5515 at 1400 K PETT to 0.5220 at 2100 K PETT.

As seen in Figure 2 (C) propulsion efficiency increases slightly with PETT and on the other hand thermal efficiency and so overall efficiency reduce with PETT.

As shown in Figure 2 (D), sT is 262.4 [m/s] and SFC is 77.970 [g/(kN.s)] at 1500 K PETT and at 2100 K PETT, performance reduce to 236.3 [m/s] for sT and 86.583 [g/(kN.s)] for SFC at sea level. ST is 361.0 [m/s] and SFC is 69.326 [g/(kN.s)] at 1500 K PETT and at 2100 K PETT, performance reduce to 334.9 [m/s] for sT and 74.728 [g/(kN.s)] for SFC at 5 km altitude.

Two design objectives (sT-SFC) change compatible with each other depending on PETT as shown in Figure 2 (D). Although low PETT values are desirable in terms of performance, it is possible to reduce the PETT to the point where there is no fuel flow.

3.2. Turbine Total Pressure Ratio Effect on Engine Performance

sT increase and SFC reduce with π_t reduce as shown in Figures 3 (A) and 3 (B) this situation shows that reduce π_t increase performance. However, to reduce π_t , it is required that turbomachinery that has more stage and therefore engine have more weight and more complex design and this situation is not desirable for engine design.

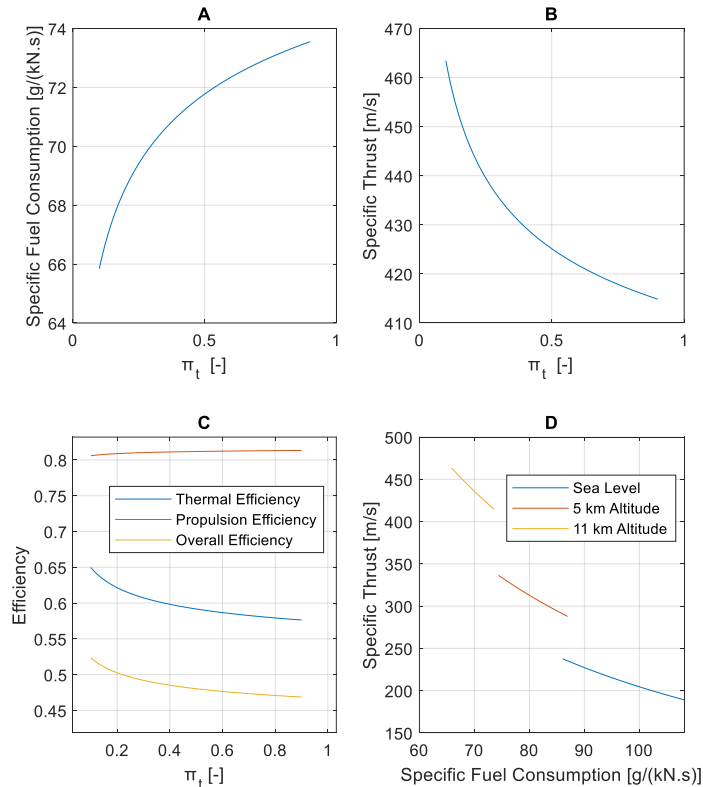


Figure 3. (A) SFC changes with π_t change (B) sT change with π_t change (C) Engine efficiencies change with π_t change (D) sT-SFC change with π_t change at different altitudes

As can be observed in Figure 3 (A), the SFC increase from 65.842 [g/(kN.s)] at 0.1 π_t to 73.551 [g/(kN.s)] at 0.9 π_t . The sT decrease from 463.4 [m/s] at 0.1 π_t to 414.9 [m/s] at 0.9 π_t as shown in Figure 3 (B).

As seen in Figure 3 (C), the propulsion efficiency slightly increase from 0.8059 at 0.1 π_t to 0.8132 at 0.9 π_t . Thermal efficiency is 0.6498 at 0.1 π_t and decreases to 0.5764 at 0.9 π_t . The overall efficiency decreases from 0.5236 at 0.1 π_t to 0.4637 at 0.9 turbine total pressure ratio.

As seen in Figure 3 (C) propulsion efficiency increases slightly with π_t and on the other hand thermal efficiency and so overall efficiency reduce with π_t similar PETT effect on efficiency.

As seen in Figure 3 (D), sT is 237.7 [m/s] and SFC is 86.051 [g/(kN.s)] at 0.1 π_t and performance reduce to 189.1 [m/s] for sT and 108.15 [g/(kN.s)] for SFC 0.9 π_t at sea level. ST is 336.4 [m/s] and SFC is 74.404 [g/(kN.s)] at 0.1 π_t and at 0.9 π_t , performance reduce to 287.8 [m/s] for sT and 86.961 [g/(kN.s)] for SFC at 5 km altitude.

As observed in Figure 3 (D), the two design objectives (ST-SFC) change compatible with each other dependent on π_t . Although low π_t are desirable, this parameter is limited by the requirement that the temperature at the exit the cooling section must not drop below a certain value.

3.3. $T_{cooling}$ Effect on Engine Performance

ST and SFC increase with $T_{cooling}$ increase as shown in Figures 4 (A) and 4 (B) and this situation shows that lower values of $T_{cooling}$ is advantage for SFC objective and higher values $T_{cooling}$ has advantage for sT objective. Therefore, the tradeoff between the two design objectives, SFC and sT, should be made based on $T_{cooling}$.

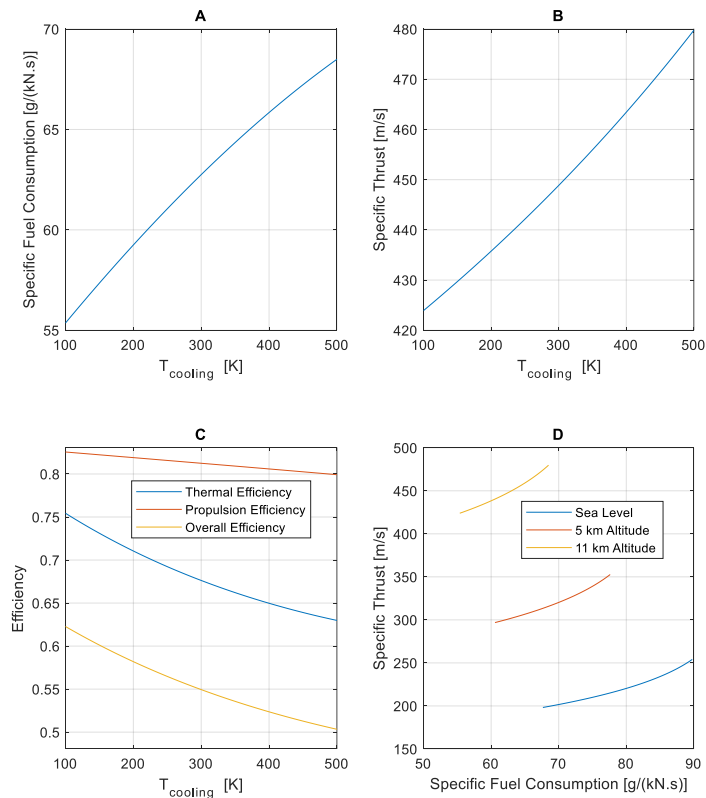


Figure 4. (A) SFC changes with $T_{cooling}$ change (B) sT change with $T_{cooling}$ change (C) Engine efficiencies change with $T_{cooling}$ change (D) sT-SFC change with $T_{cooling}$

As observed in Figure 4 (A) SFC increase from 55.360 [g/(kN.s)] at 100 K $T_{cooling}$ to 68.495 [g/(kN.s)] at 500 K $T_{cooling}$. It is observed that sT increases from 423.9 [m/s] at 100 $T_{cooling}$ to 479.8 [m/s] at 500 K $T_{cooling}$ (as seen in Figure 4 (B)).

Overall engine efficiency change from 0.6228 to 0.5033, propulsion efficiency change from 0.8255 to 0.7992, and thermal efficiency change from 0.7544 to 0.6298 as $T_{cooling}$ change from 100 K to 500 K as seen in Figure 4 (C).

As seen in Figure 4 (D), sT is 198.2 [m/s] and SFC is 67.672 [g/(kN.s)] at 100 K $T_{cooling}$ and performance change to 254.1 [m/s] for sT and 89.763 [g/(kN.s)] for SFC 500 K $T_{cooling}$ at sea level. sT is 269.9 [m/s] and SFC is 60.756 [g/(kN.s)] at 100 K $T_{cooling}$, and at 500 K $T_{cooling}$, performance change to 352.7 [m/s] for sT and 77.617 [g/(kN.s)] for SFC at 5 km altitude.

The two design objectives are in conflict with $T_{cooling}$ as can be seen in Figure 4 (D). This is because as the SFC increases, the sT value also increases. $T_{cooling}$ is limited not only by the capacity of the heat exchanger but also by the Pareto optimum of the design objectives.

Propulsion efficiency reduce slightly and thermal efficiency and so the overall pressure ratio decrease strongly with increase $T_{cooling}$ as observed in Figure 4 (C).

3.4. AETT Effect on Engine Performance

ST increase and SFC reduce with AETT increase as shown in Figures 5 (A) and 5 (B) and this situation shows that increases in AETT increases performance. However, increase in AETT is limited by the material resistance limit to temperature.

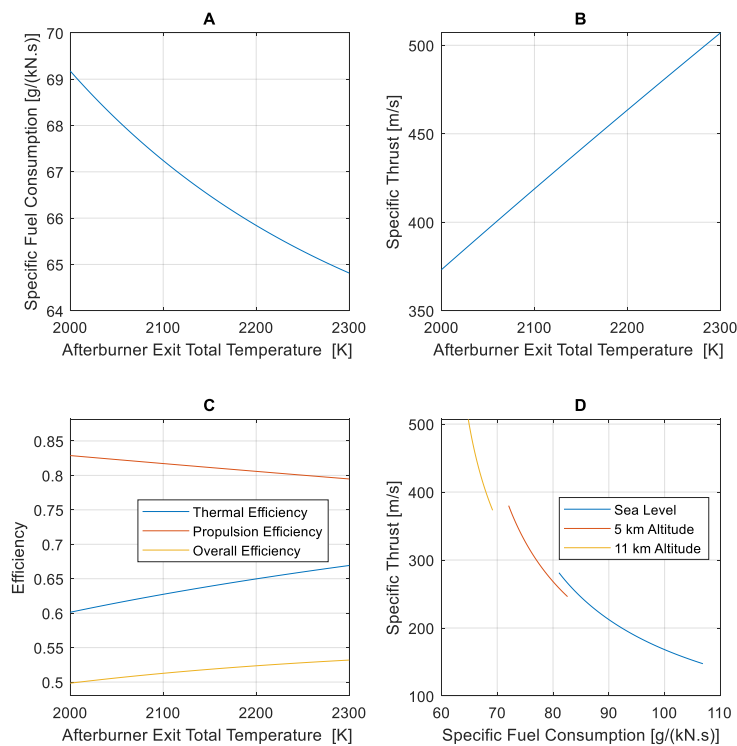


Figure 5. (A) SFC changes with AETT change (B) sT change with AETT change (C) Engine efficiencies change with AETT section (D) sT-SFC change with AETT at different altitudes

As can be seen in Figure 5 (A) the SFC reduces from 69.178 [g/(kN.s)] at 2000 K AETT to 64.814 [g/(kN.s)] at 2300 K AETT . It is observed in Figure 5 (B) that sT increases from 373.2 [m/s] at 2000 K AETT to 507.0 [m/s] at 2300 K AETT.

Overall engine efficiency increases from 0.4984 to 0.5319, propulsion efficiency reduces from 0.8288 to 0.7948 and thermal efficiency increases from 0.6013 to 0.6692 as AETT increase from 2000 K to 2300 K as seen in Figure 5 (C).

As observed in Figure 5 (D), sT is 147.5 [m/s] and SFC is 106.86 [g/(kN.s)] at 2000 K AETT and the performance changes to 281.3 [m/s] for sT and 81.068 [g/(kN.s)] for SFC at 2300 K AETT at sea level. Performance change from ST is 246.1 [m/s] and SFC is 82.601 [g/(kN.s)] at 2000 K AETT, to 380.0 [m/s] for sT and 72.050 [g/(kN.s)] for SFC at 2300 K AETT ,at 5 km altitude

Figure 5 (D) shows that SFC decreases with increasing sT. Although high AETT values are desired, it is known that this parameter is limited by the material temperature resistance.

3. 5. Coupled Parameters Effects on Engine Performance

The changes of sT and SFC depending on the turbine total pressure ratio and the total temperature decrease in the cooling section are illustrated in Figures 6 and 7, respectively. The high total temperature decrease in the cooling section and low turbine total pressure ratio values are advantageous in terms of sT. The high total temperature decrease value in the cooling section and the low turbine total pressure ratio values are advantageous in terms of SFC.

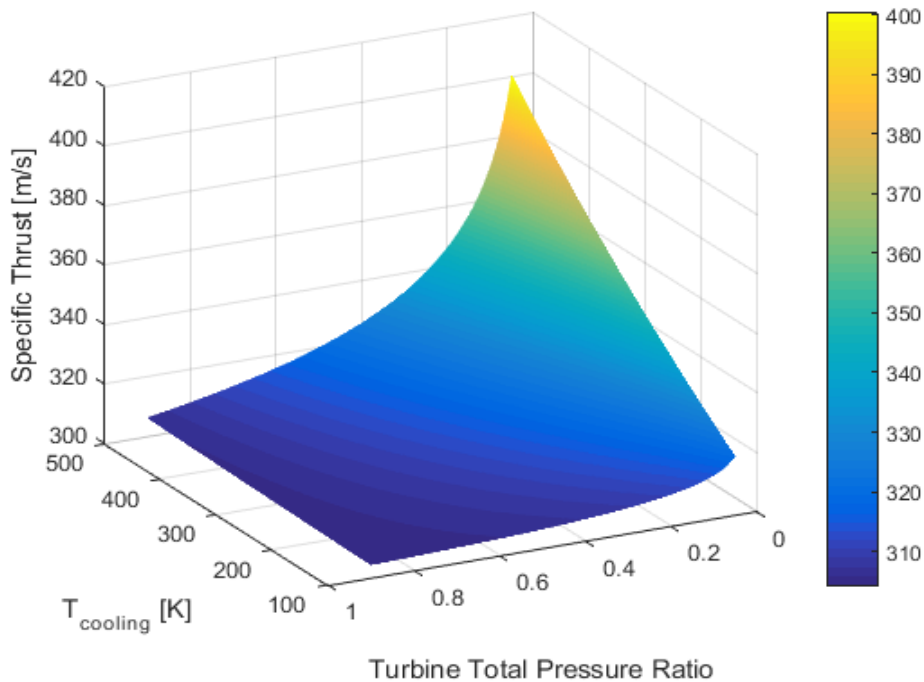


Figure 6. Change of sT dependent on turbine total pressure ratio and total temperature decrease at cooling section

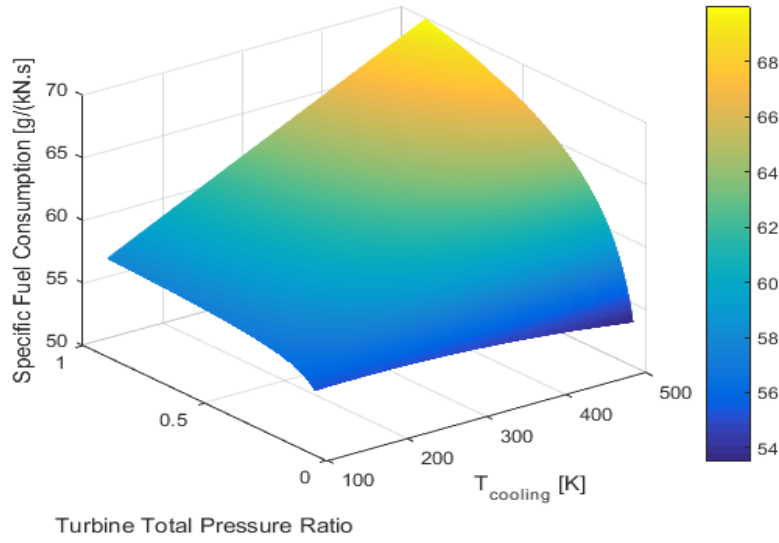


Figure 7. Change of SFC dependent on turbine total pressure ratio and total temperature decrease at cooling section π_t

4. OPTIMIZATION METHOD

Optimization is performed using the design parameters that are expressed in Table 2, based on the design conditions that are expressed in Table 2.

Table 2. Design specifications

Specifications	Parameters
Design Parameters	PETT
	π_t
	$T_{cooling}$ AETT
Design Conditions	Flight Mach Number Atmosphere Pressure Atmosphere Temperature
Parameters Dependent on Design Parameters	sT SFC Compressor Pressure Ratio
Design Objectives	sT SFC
Constraints	SFC < 55 g/kN. s Compressor Exit Total Temperature < 1000 K

Parameters dependent on the design parameters are expressed at Table 2. Parameters are dependent on design parameters and two of parameters dependent on design parameters are selected as design objectives as expressed in Table 2. One parameter dependent on the design parameters, compressor exit total temperature, is used as a constraint, as expressed in Table 2. Two design objectives are ranked based on design objective priority and based on this rank, one of them that is more important, sT, is used as design objective and the other one that is assumed to be less important, SFC, is used as the design constraint expressed in Table 2. The optimization parameters ranges are expressed in Table 3.

Table 3. Range of optimization parameters

Optimization Parameters	Parameter Range
PETT	1500 – 2200 K
π_t	0.1 - 0.9
$T_{coolina}$	100 - 500 K
AETT	2000 - 2300 K

The particle swarm optimization method is used in the optimization of the IBCE and the typical range of particle swarm optimization method control parameters is expressed in Table 4 [29-33].

Table 4. Particle swarm optimization algorithm control parameter typical range [33]

Parameter	Meaning	Typical Range
ω	Inertia Weight	0.8 - 1.2
c_1	Cognition Learning Rate	0 - 4
c_2	Social Learning Rate	0 - 4
N	Number of Particles	20 - 40

The optimization parameter values expressed in Table 5 are obtained by using the values in the mean of the typical range of particle swarm optimization method control parameters expressed in Table 4. In the particle swarm optimization of the IBCE, the optimization control parameters expressed in Table 5 are used in this study.

Table 5 Particle swarm optimization algorithm control parameter values

Parameter	Meaning	Value
ω	Inertia Weight	1
c_1	Cognition Learning Rate	2
c_2	Social Learning Rate	2
N	Number of Particles	30

The optimization algorithm is expressed basically in Figure 12 based on information expressed in Tables 5 and 6.

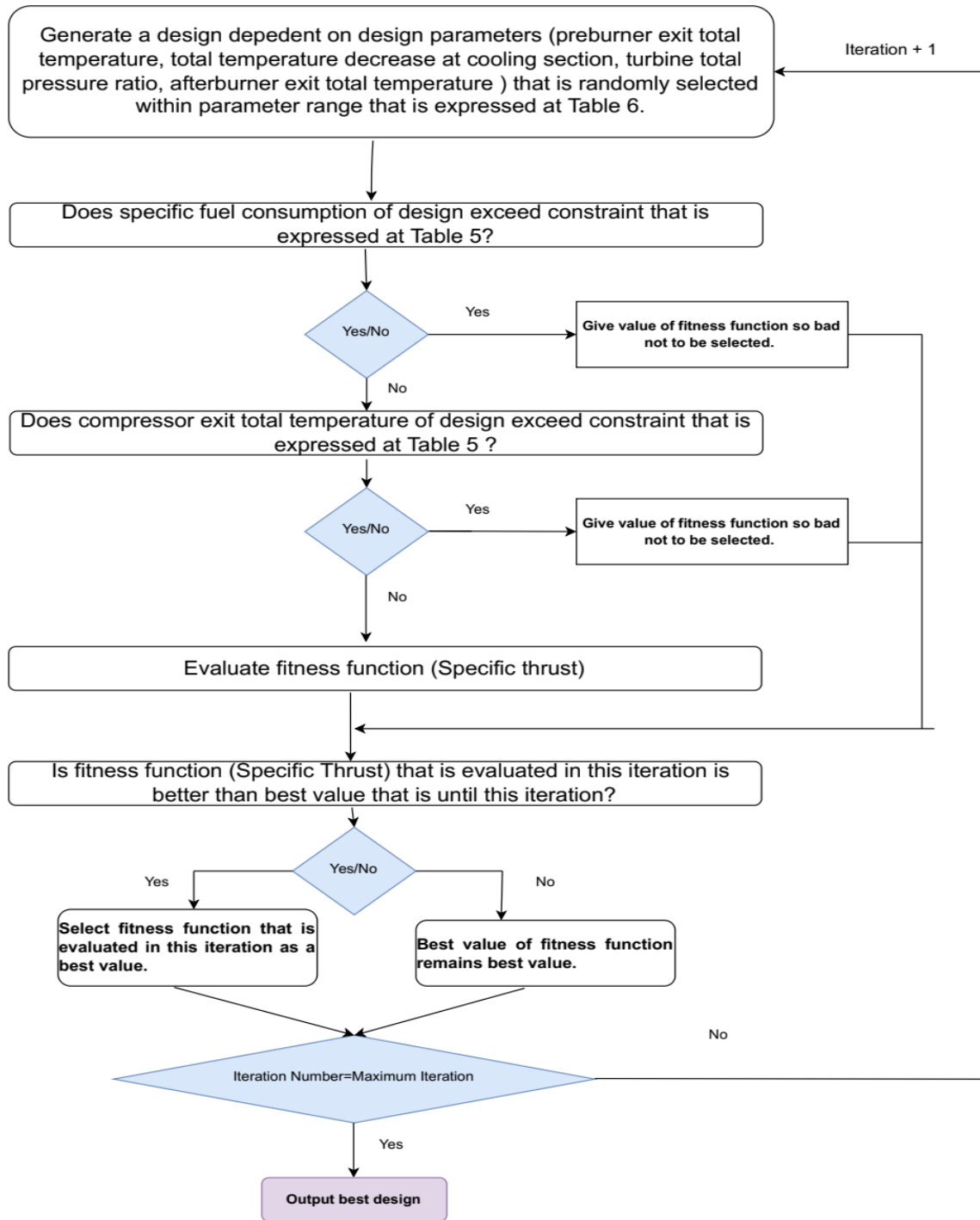


Figure 12. Optimization algorithm flowchart

5. RESULTS

The change of the optimum value of the design objective, sT and the optimum design parameters in optimization with each iteration are expressed Figure 13 and Figure 14, respectively.

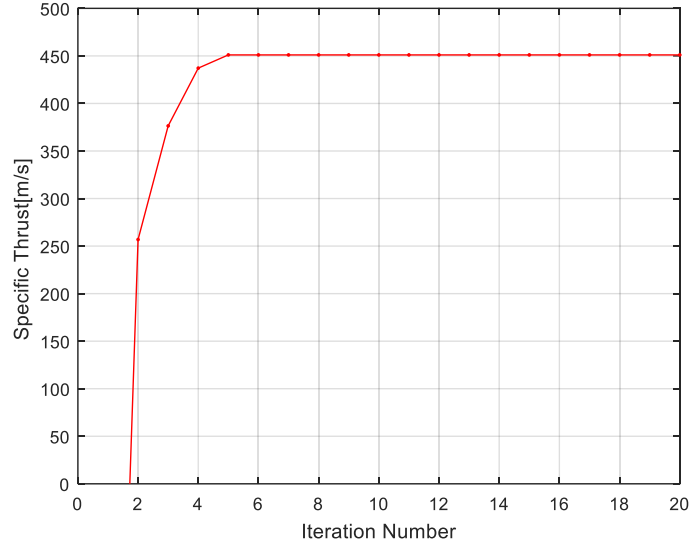


Figure 21. The change of optimum design objective obtained by optimization using genetic algorithms with each iteration

The optimization results of IBCE are given in Table 12. The optimum design parameters obtained as a result of the optimization of the IBCE are given in Table 13.

Table 12. Optimization Results

Optimization Characteristics	Parameter	Value
Optimization Objective	sT [N.s/kg]	451.052
Optimization Constraints	SFC [g/kN.s]	1000
	Compressor Exit Total Temperature [K]	276.9
	Cooling Section Exit Total Temperature [K]	

Table 13. The optimum values of design parameters for sT optimization

Optimization Parameters	Optimum
PETT	1500 K
π_t	0.1
$T_{cooling}$	500 K
AETT	2300 K

6. CONCLUSION

When the total temperature of the cooling section is examined, it is seen that a temperature above the freezing temperature of the air is obtained. A very high sT value is obtained at the hypersonic flight Mach Number (5 Mach) as a result of optimization. Concluded that IBCE is expected to be a candidate for hypersonic flight. There are concluded that:

- SFC reduces % 5.3 and sT increases % 5.6 dependent on PETT change from 2100 K to 1400 K.
- Based on $T_{cooling}$ change from 100 K to 500 K, it is observed that SFC increases %23.7 and sT increases % 13.1.
- It is observed that SFC reduces % 6.3 and sT increases % 35.9 dependent on AETT change from 2000 K to 2300 K.
- SFC reduces % 10.5 and sT increases % 11.7 dependent on π_t change from 0.9 to 0.1.
- Temperature decrease with increasing altitude effect performance dramatically as positive.
- Low PETT values are desirable in terms of performance.
- High AETT values are desired, so increasing material temperature with the development of technology positively effects performance.
- The two design objectives are in conflict with the total temperature decrease at cooling section. Total temperature decrease at cooling section increasing effect sT performance positively and effect SFC negatively.
- Low turbine total temperature ratio values are desirable for two design objectives (sT-SFC) but this parameter is limited by the requirement that the temperature at the exit the cooling section must not drop below a certain value

Heat exchanger efficiency and pressure losses can be determined by conceptual and CFD investigations. After heat exchanger efficiency and pressure losses will be determined real IBCE cycle analysis can be performed. Optimization can be performed based on the real cycle analysis of IBCE. The relationship between the design parameters and the performance of IBCE can be shown based on real cycle analysis.

CONFLICT OF INTEREST

The authors declare that they have no known competing financial interests or personal relationships that could have appeared to influence the work reported in this paper.

AUTHORSHIP CONTRIBUTIONS

Authors contributed equally to the study

Mustafa Karabacak: Software, Methodology, Writing- Reviewing and Editing, Validation; **Onder Turan:** Supervision, Conceptualization, Writing- Reviewing and Editing. The corresponding author **Mustafa Karabacak**, is responsible for ensuring that the descriptions are accurate and agreed by all authors.

REFERENCES

- [1] Cross N, Cross AC. Expertise in engineering design. Research in engineering design 1998; 10(3): 141-149.
- [2] Haik Y, Sivaloganathan S, Shahin, TM. Engineering design process. Cengage Learning 2015.
- [3] Hubka V. Principles of engineering design. Elsevier 2015.
- [4] Buede DM, Miller WD. The engineering design of systems: models and methods 2016.
- [5] Cross N. Engineering design methods: strategies for product design. John Wiley & Sons 2021.
- [6] Bianchi M, Negri di Montenegro G, Peretto A, Spina, PR. A feasibility study of inverted Brayton cycle for gas turbine repowering. J. Eng. Gas Turbines Power 2005; 127(3):599-605.

- [7] Farokhi S. Aircraft propulsion. John Wiley & Sons 2014.
- [8] Kurzke J. GasTurb 13: design and off-design performance of gas turbines. Aachen: GasTurb GmbH 2021.
- [9] Mattingly JD, Heiser WH, Pratt DT. Aircraft engine design. American Institute of Aeronautics and Astronautics 2002.
- [10] Pennington WA. Choice of engines for aircraft. Shell Aviation News. January 1959; 14–19 .
- [11] Raymer D. Aircraft design: A conceptual approach. AIAA 1989; 233–236.
- [12] Kyprianidis KG, Rolt AM, Grönstedt T. Multi-disciplinary analysis of a geared fan intercooled core aero-engine. In Turbo Expo: Power for Land, Sea, and Air, 2013; 55133: V002T07A027.
- [13] Kyprianidis KG, Rolt AM. On the optimisation of a geared fan intercooled core engine design. In Turbo Expo: Power for Land, Sea, and Air. 2014;45653: V03AT07A018.
- [14] Sato T, Tanatsugu N, Naruo Y, Omi J, Tomike JI, Nishino T. Development study on ATREX engine. Acta Astronautica 2000; 47(11): 799-808.
- [15] Webber H, Bond A, Hempzell M. Sensitivity of pre-cooled air-breathing engine performance to heat exchanger design parameters. In 57th International Astronautical Congress, 2006; D2-P.
- [16] Dong P, Tang H, Chen M. Study on multi-cycle coupling mechanism of hypersonic precooled combined cycle engine. Applied Thermal Engineering 2018; 131: 497-506.
- [17] Yu X, Wang C, Yu D. Thermodynamic design and optimization of the multi-branch closed Brayton cycle based precooling-compression system for a novel hypersonic aeroengine. Energy Conversion and Management 2020; 205: 112412.
- [18] Murray JJ, Guha A, Bond A. Overview of the development of heat exchangers for use in air-breathing propulsion pre-coolers. Acta astronautica 1997; 41(11): 723-729.
- [19] Di Battista D, Fatigati F, Carapellucci R, Cipollone R. Inverted Brayton Cycle for waste heat recovery in reciprocating internal combustion engines. Applied Energy 2019; 253(113565).
- [20] Kennedy I, Chen Z, Ceen B, Jones S, Copeland CD. Experimental investigation of an inverted Brayton cycle for exhaust gas energy recovery. Journal of Engineering for Gas Turbines and Power 2019; 141(3).
- [21] Huang W, Du ZB, Yan L, Xia ZX. Supersonic mixing in airbreathing propulsion systems for hypersonic flights. Progress in Aerospace Sciences 2019; 109(100545).
- [22] Huang W, Pourkashanian M, Ma L, Ingham DB, Luo SB, Wang ZG. Investigation on the flame holding mechanisms in supersonic flows: backward-facing step and cavity flameholder. Journal of Visualization 2011; 14: 63-74.
- [23] Khan A, Akram S, Kumar R. Experimental study on enhancement of supersonic twin-jet mixing by vortex generators. Aerospace Science and Technology 2020; 96(105521).

- [24] Verma KA, Pandey KM, Sharma KK. Study of Fuel Injection Systems in Scramjet Engine—A Review. *Recent Advances in Mechanical Engineering: Select Proceedings of ICRAME, 2021; 2020: 931-940.*
- [25] Verma KA, Kapayeva S, Pandey KM, Sharma KK. The recent development of supersonic combustion ramjet engines for augmentation of the mixing performance and improvement in combustion Efficiency: A review. *Materials Today: Proceedings 2021; 45: 7058-7062.*
- [26] Verma KA, Pandey KM, Ray M, Sharma KK. Effect of transverse fuel injection system on combustion efficiency in scramjet combustor. *Energy 2021; 218(119511).*
- [27] Zhang W, Chen L, Sun F, Wu C. Second-law analysis and optimisation for combined Brayton and inverse Brayton cycles. *International Journal of Ambient Energy 2007; 28(1): 15-26.*
- [28] Tsujikawa Y, Kaneko KI, Tokumoto S. Inverted Turbo-Jet Engine for Hypersonic Propulsion. In *Turbo Expo: Power for Land, Sea and Air, 2005; 47284: 343-349.*
- [29] Kennedy J, Eberhart R. Particle swarm optimization. In *Proceedings of ICNN'95-international conference on neural networks IEEE, 1995; 4:1942-1948.*
- [30] Poli R, Kennedy J, Blackwell T. Particle swarm optimization. *Swarm intelligence 2007; 1(1): 33-57.*
- [31] Hu X, Eberhart R. Multiobjective optimization using dynamic neighborhood particle swarm optimization. In *Proceedings of the 2002 Congress on Evolutionary Computation. CEC'02, 2002; 2: 1677-1681.*
- [32] Hu X. Particle Swarm Optimization. <http://www.swarmintelligence.org> [Online: accessed 16-May-2016]
- [33] Beltrán-Prieto JC, Komínková Oplatková Z, Torres Friás R, Escoto Hernández JL. A time performance comparison of particle swarm optimization in mobile devices. In *MATEC Web of Conferences 20th International Conference on Circuits, Systems, Communications and Computers (CSCC 2016). EDP Sciences, 2016.*